crystals

Article

Mechanical and Thermal Dehydrogenation of Lithium Alanate (LiAlH$_4$) and Lithium Amide (LiNH$_2$) Hydride Composites

Robert A. Varin [1],* and Leszek Zbroniec [2]

[1] Department of Mechanical and Mechatronics Engineering, University of Waterloo, 200 University Ave. W., N2L 3G1, Waterloo, Ontario, Canada

[2] Wroclaw Research Centre EIT+, Stablowicka 147, 54-066 Wroclaw, Poland;
E-Mail: Leszek.Zbroniec@hotmail.com

* Author to whom correspondence should be addressed; E-Mail: ravarin@uwaterloo.ca;
Tel./Fax: +1-519-885-5862.

Abstract: Hydrogen storage properties of the (nLiAlH$_4$ + LiNH$_2$) hydride composite where $n = 1, 3, 11.5$ and 30, synthesized by high energy ball milling have been investigated. The composite with the molar ratio $n = 1$ releases large quantities of H$_2$ (up to ~5 wt.%) during ball milling up to 100–150 min. The quantity of released H$_2$ rapidly decreases for the molar ratio $n = 3$ and is not observed for $n = 11.5$ and 30. The XRD studies indicate that the H$_2$ release is a result of a solid state decomposition of LiAlH$_4$ into (1/3)Li$_3$AlH$_6$ + (2/3)Al + H$_2$ and subsequently decomposition of (1/3)Li$_3$AlH$_6$ into LiH + (1/3)Al + 0.5H$_2$. Apparently, LiAlH$_4$ is profoundly destabilized during ball milling by the presence of a large quantity of LiNH$_2$ (37.7 wt.%) in the $n = 1$ composite. The rate of dehydrogenation at 100–170 ℃ (at 1 bar H$_2$) is adversely affected by insufficient microstructural refinement, as observed for the $n = 1$ composite, which was milled for only 2 min to avoid H$_2$ discharge during milling. XRD studies show that isothermal dehydrogenation of (nLiAlH$_4$ + LiNH$_2$) occurs by the same LiAlH$_4$ decomposition reactions as those found during ball milling. The ball milled $n = 1$ composite stored under Ar at 80 ℃ slowly discharges large quantities of H$_2$ approaching 3.5 wt.% after 8 days of storage.

Keywords: solid state hydrogen storage; lithium alanate; lithium amide; ball milling; mechanical and thermal dehydrogenation

1. Introduction

In the last few decades, hydrogen has been perceived as a future energy carrier that may allow a gradual transformation from a fossil fuel-based economy to a hydrogen economy. An important obstacle to the implementation of a widespread hydrogen economy is the development of an efficient hydrogen storage technology for various industrial sectors, and particularly for transportation/automotive applications. Gaseous and liquid hydrogen storage techniques have a number of serious drawbacks, although high pressure (70 MPa) gaseous storage will, most likely, be a short-term solution for the automotive sector. However, for stationary, portable and off-road mobile applications as well as for long-term automotive applications, a general consensus has emerged that a better option is solid state hydrogen storage in hydrides and their composite systems. Due to the specific requirements of Proton Exchange Membrane (PEM) fuel cell stacks which are the most suitable for automotive and a number of other applications, a potential hydride-based storage system should have the operating temperature of dehydrogenation compatible with waste heat of a PEM fuel cell stack, which roughly means a temperature range not exceeding 70–100 °C. Obviously, the highest possible H_2 capacity of the solid hydride storage system is another important consideration, and the recently revised US Department of Energy (DOE) automotive targets for 2015 require a H_2 capacity of 5.5 wt.% for the entire storage system, which includes storage medium, tank and some auxiliary devices [1]. This translates into approximately ~10 wt.% H_2 capacity for the solid hydride-based storage material. Such large capacities can be provided by complex light metal/nonmetal hydrides and most likely by their composites [2].

One high capacity hydride composite is the $LiAlH_4$-$LiNH_2$ (lithium alanate-lithium amide) system. $LiAlH_4$ has a theoretical H_2 capacity of about 10.6 wt.%. However, the useful theoretical capacity accessible below 250 °C is about 7.9 wt.% H_2, since the rest is attributed to the dehydrogenation of LiH which only decomposes at temperatures >300 °C [2]. $LiNH_2$ composited with LiH has a theoretical H_2 capacity of about 9.8 wt.% although the accessible quantity at reasonably low temperatures is about 6 wt.% H_2 [2]. By combining two high H_2 capacity hydrides there is a potential to achieve a composite that might have higher accessible H_2 capacity than each constituent in isolation. The $LiAlH_4$-$LiNH_2$ hydride system has been investigated in the past five years, but not very systematically. There are some contradictory findings reported in the literature, most likely related to the fact that the system has a tendency to decompose during processing by ball milling, releasing hydrogen. Lu and Fang [3], Chen *et al.* [4], Naik *et al.* [5] and Dolotko *et al.* [6] used simple mixing rather than milling of the two constituents, $LiAlH_4$ and $LiNH_2$. The thermal dehydrogenation of the mixture was investigated by thermogravimetric analysis (TGA) combined with X-ray diffraction (XRD) and other techniques. It should be pointed out that processing by mixing only leads to loosely-bonded powder particles of constituents rather than a real hydride composite. The synthesis of composite requires more energetic ball milling in order to induce an alloying of the phases within particles, an intimate contact between constituent particles and a simultaneous reduction of the particle size and the size of crystallites (grains) within the particles [2]. Xiong *et al.* [7, 8], Nakamori *et al.* [9] and Dolotko *et al.* [10] were the first to report decomposition of the composites (1$LiAlH_4$ + $LiNH_2$) (molar ratio 1:1) and (0.5$LiAlH_4$ + $LiNH_2$) (1:2) during ball milling. Formation of an intermediate hydride phase $Li_3AlN_2H_4$ or the AlN compound was reported by Xiong *et al.* [7, 8] and Dolotko *et al.*

[10], respectively. The former authors also suggested that an intermediate hydride phase $Li_3AlN_2H_4$, transformed at about 500 ℃ to Li_3AlN_2 giving a total capacity of 9.5 wt.% H_2. None of these references reported systematic studies of the effect of molar ratio $LiAlH_4$ to $LiNH_2$ on behavior during ball milling and ball milling conditions on subsequent mechanical and thermal dehydrogenation. The present study addresses all these issues.

2. Experimental Method

Hydride powders of $LiAlH_4$ (97% purity) and $LiNH_2$ (purity 95%), were mixed in the following molar ratios: $n = 1, 3, 11.5$ and 30 $LiAlH_4$. The molar ratio 11.5 corresponds exactly to 5 wt.% $LiNH_2$ content. The hydride powder mixtures with the ball-to-powder weight ratio R = 132 were subsequently processed by controlled ball milling for selected time durations in the magneto-mill Uni-Ball-Mill 5 under IMP68 mode. This is a high impact energy mode with two very strong Nd-Fe-B magnets at the 6 and 8 o'clock positions and 4 steel balls (each 25 mm in diameter) in the vial [2, 11–15]. The pressure of high purity hydrogen (purity 99.999%: $O_2 < 2$ ppm; $H_2O < 3$ ppm; $CO_2 < 1$ ppm; $N_2 < 6$ ppm; CO < 1 ppm; THC < 1 ppm) in the vial was kept constant at ~600 kPa during the entire milling process. Ball milling was carried out under continuous cooling of the milling vial by an air fan. The release of hydrogen during ball milling was estimated from the pressure increase in the milling vial measured by a pressure gauge using the ideal gas law [2] and expressed in wt.% with respect to the total weight of powder sample. The handling was carried out in a glove box containing a Drierite granulated compound removing moisture. Before handling, the glove box was purged a few times and then filled with high purity argon gas (99.999% purity) in order to minimize any possible contamination by moisture or oxygen from the air.

The hydrogen thermal desorption was evaluated using a second generation volumetric Sieverts-type apparatus, custom-built by A.O.C. Scientific Engineering Pty Ltd., Australia [2]. This apparatus built entirely of austenitic stainless steel allows loading of a powder sample into a stainless steel reactor in a glove box under high purity argon and its subsequent transfer to the main unit in a sealed reactor without any exposure to the environment. Approximately 20–30 mg of sample was used in a desorption test. Before starting the desorption test, the inner tubing of the apparatus was evacuated and purged four times with argon and then twice with hydrogen. The furnace of the apparatus was heated separately to the desired test temperature and subsequently inserted onto a tightly sealed powder sample reactor inside which an atmospheric pressure of 1 bar H_2 (0.1 MPa H_2) was kept. Hence, the beginning of the desorption test was in reality pseudo-isothermal before the powder sample temperature reached the desired value. However, the calibrated time interval within which the powder sample in the reactor reaches the furnace temperature is on the order of 400 s in the 100–200 ℃ range, which is small compared to the desorption completion time making the test nearly "isothermal". Desorption curves were corrected for the hydrogen gas expansion due to the increase in temperature. The amount of desorbed hydrogen was calculated from the ideal gas law as described in detail in [2] and expressed in wt.% with respect to the total weight of powder sample. The calibrated accuracy of desorbed hydrogen capacity is about ±0.1 wt.% H_2 and that of temperature reading and stabilization ±0.1 ℃. X-ray powder diffraction (XRD) analysis was performed on a Bruker D8 diffractometer using a monochromated $CuK_{\alpha}1$ radiation ($\lambda = 0.15406$ nm) produced at an accelerating voltage of 40 kV and

a current of 30 mA. The scan range was from $2\theta = 10\,°$ to $90\,°$ and the rate was $1.2\,°\,\text{min}^{-1}$ with a step size of $0.02\,°$. Powder was loaded into a home-made XRD environmental brass holder with a glass/Cu plate for powder support in a glove box filled with Ar. The upper and lower parts of the XRD environmental holder are sealed through a soft-rubber O-ring and tightened using threaded steel bolts with nuts. The upper part of the holder contains a Kapton window transmittable to X-rays.

3. Results and Discussion

Figure 1a shows the quantity of H_2 desorbed during ball milling, plotted as a function of the molar ratio n in the (nLiAlH$_4$ + LiNH$_2$) composite. It is observed that during ball milling up to 30 min., the composites with molar ratios $n = 1$ and 3 gradually release H_2. In particular, Figure 1b shows that for $n = 1$ further ball milling up to 100–150 min releases as much as 5 wt.% H_2. We repeated the milling test in Figure 1b twice (1st and 2nd run) to confirm that the results are reproducible. As can be seen, the hydrogen desorption during ball milling for the composite with $n = 1$ is perfectly reproducible and the quantity of desorbed H_2 is nearly exactly the same for the 1st and 2nd run. Also, Figure 1a shows that the composites with $n = 11.5$ and greater do not release hydrogen during milling up to 30 min.

Figure 1. The quantity of H_2 desorbed during ball milling for (nLiAlH$_4$ + LiNH$_2$) as a function of (**a**) the molar ratio n (the numbers show the corresponding values of n) and (**b**) milling time for the composite with $n = 1$.
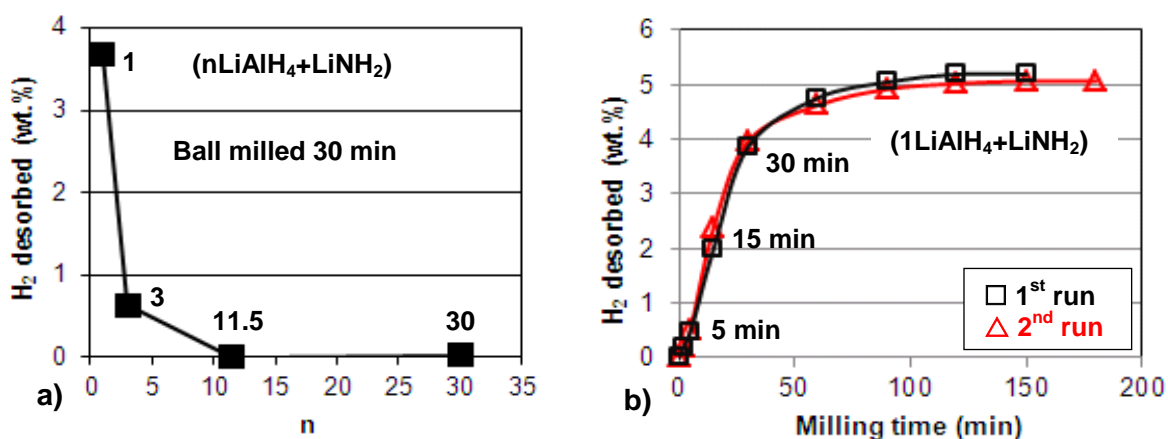
In order to obtain more insight into the phase changes occurring during ball milling as a function of milling time and molar ratio, X-ray diffraction (XRD) tests were carried out on the composite samples extracted after pre-determined milling durations. The XRD patterns are shown in Figure 2. The XRD pattern for the $n = 1$ composite (Figure 2a) shows that after 2 min of milling the diffraction peaks of both constituents LiAlH$_4$ and LiNH$_2$ are still clearly observed. There is also a peak of Al which is an impurity in as received LiAlH$_4$ [11, 12]. After 15 min of ball milling, the principal peaks of Li$_3$AlH$_6$ appear and the principal Al peak becomes stronger, indicating that more Al is formed during milling. It must be pointed out that the presence of the strong diffraction peaks of LiNH$_2$ indicates that no chemical reaction between LiAlH$_4$ and LiNH$_2$ occurred during ball milling.
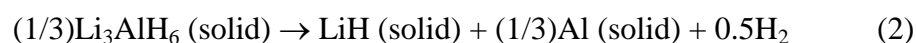
Figure 2. XRD patterns for (**a**) (1LiAlH$_4$ + LiNH$_2$) after milling for 2 and 15 min, (**b**) (1LiAlH$_4$ + LiNH$_2$) after milling for 30 min, 1 h and 3 h, and (**c**) (3LiAlH$_4$ + LiNH$_2$) after milling for 2 and 15 min. The ICDD file numbers for phase identification are shown in the legend.
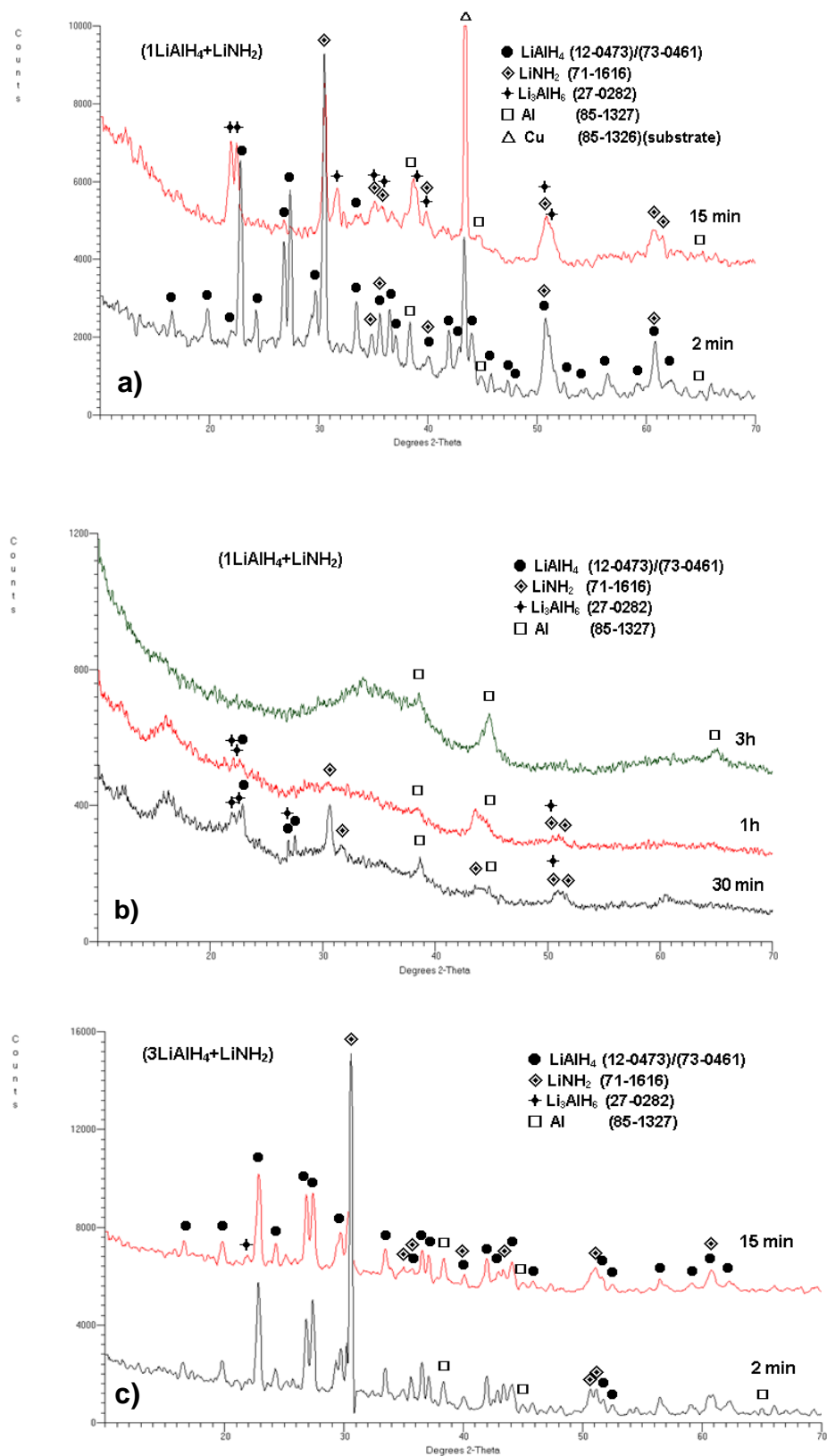
As can be seen in Figure 2b for the *n* = 1 composite, with increasing ball milling time to 30 min, 1 h and 3 h, the peaks become broadened and diffused as well as a pronounced rise in the baselines and the formation of a broad "hump" in the range of 2θ = 30–40 ° are observed, which can be attributed to heavy nanostructuring or even the existence of increasing quantities of amorphous structure(s) [7, 8]. The 100% intensity peaks of $LiAlH_4$, $LiNH_2$ and Li_3AlH_6 are still visible after 30 min and even after 1 h of milling although much weakened (Figure 2b). There are also clear peaks which we assign to Al. It is interesting that Xiong *et al.* [7], in their first paper on the ball milling of ($1LiAlH_4$ + $LiNH_2$)(molar ratio *n* = 1) reported that the peaks of Al were clearly observed in the XRD patterns of the ball milled samples, although they were gradually weakened with milling time. However, in their second paper [8] on the ball milling of ($0.5LiAlH_4$ + $LiNH_2$)(molar ratio *n* = 0.5) they reported that no Al peaks were detected during the milling process. In contrast, Dolotko *et al.* [10] reported that no Al was detected in the ($1LiAlH_4$ + $LiNH_2$) composite during ball milling but instead they concluded that the amorphous AlN compound was formed during ball milling. On that basis, they proposed that a solid state reaction between $LiAlH_4$ and $LiNH_2$ occurred during ball milling which resulted in the formation of AlN, 2LiH and $2H_2$. The quantity of H_2 released in this transformation is 6.6 wt.% which they claimed to be released after 30 min of ball milling.

However, we believe that the peaks assigned to Al in Figure 2a, b for the milling duration from 2 min to 1 h of milling, indeed correspond to Al and not to AlN. There is some ambiguity here because the Fm3m space group of Al (ICDD 85-1327) is identical to AlN (ICDD 46-1200), which means that their XRD diffraction patterns practically superimpose. However, the intensities of the principal peaks of Al and AlN are opposite. For Al the (111) peak at 2θ = 38.5 ° and (200) peak at 2θ = 44.7 ° has 100 and 50% intensity, respectively. For AlN the intensity of (111)(2θ = 38.5 °), (200)(2θ = 44.7 °) and (220) (2θ = 65.1 °) peak is 30, 100 and 55%, respectively. The XRD patterns in Figure 2a, b show that from 2 min to 1 h of milling duration the order of intensities for the peaks assigned to Al corresponds rather unambiguously to Al. However, the order of peak intensities changes after 3 h of milling since the first peak assigned to Al in this pattern (Figure 2b) is weaker than the second one and also the third peak at around 2θ = 65 ° appears. This intensity order may correspond to AlN. However, the observed alterations in the intensities of peaks assigned to Al after 3 h milling could also, at least to some extent, be induced by severe nanostructuring/amorphization of the ball-milled composite powders. Still, the maximum desorbed quantity of 5 wt.% H_2, reproducibly observed after 3 h of milling (Figure 1b), does not support the reaction path involving the formation of AlN which requires 6.6 wt.% H_2 as claimed by Dolotko *et al.* [10]. The XRD patterns for the ($3LiAlH_4$ + $LiNH_2$) (*n* = 3) composite after ball milling for 2 and 15 min (Figure 2c) still indicate the presence of both $LiAlH_4$, $LiNH_2$ and Al, the latter being a pre-existing impurity for the composite milled for 2 min. After 15 min milling a very small principal peak of Li_3AlH_6 appears.

In general, it is well-known in the literature [2,11–13] that the dehydrogenation of $LiAlH_4$ in solid state occurs in three stages as shown below:

$$LiAlH_4 \text{ (solid)} \rightarrow (1/3)Li_3AlH_6 \text{ (solid)} + (2/3)Al \text{ (solid)} + H_2 \qquad (1)$$
$$(1/3)Li_3AlH_6 \text{ (solid)} \rightarrow LiH \text{ (solid)} + (1/3)Al \text{ (solid)} + 0.5H_2 \qquad (2)$$
$$LiH \text{ (solid)} \rightarrow Li + 0.5H_2 \text{ or } LiH + Al \rightarrow LiAl + 0.5H_2 \qquad (3)$$

Only reactions (1) and (2) are accessible for practical hydrogen storage, because they occur up to roughly 250 °C in DSC tests. Reaction (3) occurs much above 300 °C and is of no interest [2, 11–13]. Theoretical H_2 capacity of reactions (1) and (2) is 5.3 and 2.6 wt.%, respectively, which, for 97% pure $LiAlH_4$ used in this work, reduces to 5.14 and 2.52 wt.%, respectively. The composite with the molar ratio of $n = 1$ ($1LiAlH_4 + LiNH_2$) corresponds to a weight ratio of 62.3 wt.% $LiAlH_4$ and 37.7 wt.% $LiNH_2$. Therefore, at this weight ratio, fully completed reactions (1) and (2) should provide approximately purity-corrected 3.2 and 1.6 wt.% H_2, respectively. Since ~5 wt.% H_2 is released after 150 min ball milling (Figure 1b), both reactions must have occurred during ball milling. This is a very interesting observation because in a thermal DSC test, reaction (1) is exothermic and (2) is endothermic [2, 12, 13]. That would suggest that both types of reactions, thermodynamically opposite, have been realized during high energy ball milling of hydride composites in the present work. However, since during ball milling the overall temperature increase in the milling vial is very small then the question arises whether the thermodynamic character of both reactions, which are now induced by mechanical energy, remains the same as that at elevated temperatures in a DSC test.

Furthermore, it seems that the entire quantity of H_2 desorbed during ball milling for the $n = 1$ composite (Figure 1b) can be easily provided by reactions (1) and (2) without invoking other reactions as claimed by Dolotko *et al.* [10]. The fact that the diffraction peaks of $LiNH_2$ in the $n = 1$ composite persist throughout a long period of milling (Figure 2a, b) indicates that $LiNH_2$ does not react/decompose but most likely becomes heavily nanostructured or even partially amorphized, and in this capacity destabilizes $LiAlH_4$ during ball milling and enhances its decomposition according to reactions (1) and (2) without involvement of any other reactions. However, with decreasing molar content of $LiNH_2$ in the composite ($n = 3$ and larger), $LiNH_2$ somehow ceases to destabilize $LiAlH_4$ during ball milling. At the content of 5 wt.% ($n = 11.5$) no release of H_2 is observed (Figure 1b) for the applied milling time.

So far, such observations have never been reported in the literature. However, at the moment it is difficult to propose any detailed molecular mechanism by means of which $LiNH_2$ destabilizes $LiAlH_4$ during ball milling and, furthermore, the dependence of that mechanism on the molar ratio of the composite. Xiong *et al.* [7] pointed out that $LiNH_2$ may not work as a simple catalyst. They tried to get more insight into the role of $LiNH_2$ in the ($0.5LiAlH_4 + LiNH_2$) composite using Nuclear Magnetic Resonance (NMR) and Infrared Fourier Transform (FTIR) measurements. They came to the conclusion that an intermediate with the approximate chemical composition of "$Li_3AlN_2H_4$" was formed during milling. However, in their interpretation "$Li_3AlN_2H_4$" is not really a new hydride but a mixture of ($LiNH_2 + AlN + 2LiH$) - either amorphous or poorly crystalline. However, our XRD patterns in Figure 2a,b convincingly show that the peaks of $LiAlH_4$, Li_3AlH_6, $LiNH_2$ and Al are clearly observed after up to 1 h of high energy ball milling although they become progressively broader and weaker. Their persistent presence does not support the existence of any new intermediates and their broadening/weakening is quite typical for the progressive occurrence of nanostructuring/amorphization during ball milling.

Figure 3 shows volumetric isothermal dehydrogenation curves at four temperatures for ($1LiAlH_4 + LiNH_2$) ball milled for 2 min. In this case, a short milling time was used to avoid any desorption of H_2 during milling (Figure 1b). The composite is able to dehydrogenate at 100 °C,

although at a slow rate. Barely ~3 wt.% H_2 is desorbed after a very long time of 43 h. However, this quantity of H_2 is in excellent agreement with the purity-corrected H_2 capacity of reaction (1) in the $n = 1$ composite, as discussed above. This finding further supports our explanation. With increasing temperature the rate of dehydrogenation increases, as expected, but still remains relatively sluggish. Even at 170 °C about 7 h time duration is required to desorb 5 wt.% H_2. It is also seen that at 140, 150 and 170 °C dehydrogenation curves exhibit two clear stages, designated I and II in Figure 3b. Stage I always desorbs ~3 wt.% H_2 while Stage II desorbs the rest of the total quantity of H_2. Apparently, Stage I and II correspond closely to reactions (1) and (2), respectively.

Figure 3. Volumetric dehydrogenation curves at (**a**) 100 °C, (**b**) 140 °C, (**c**)150 °C and (**d**) 170 °C (at 1 bar H_2) for ($1LiAlH_4 + LiNH_2$) ball milled for 2 min. The arrows indicate the end time of dehydrogenation after which samples were taken for XRD tests.
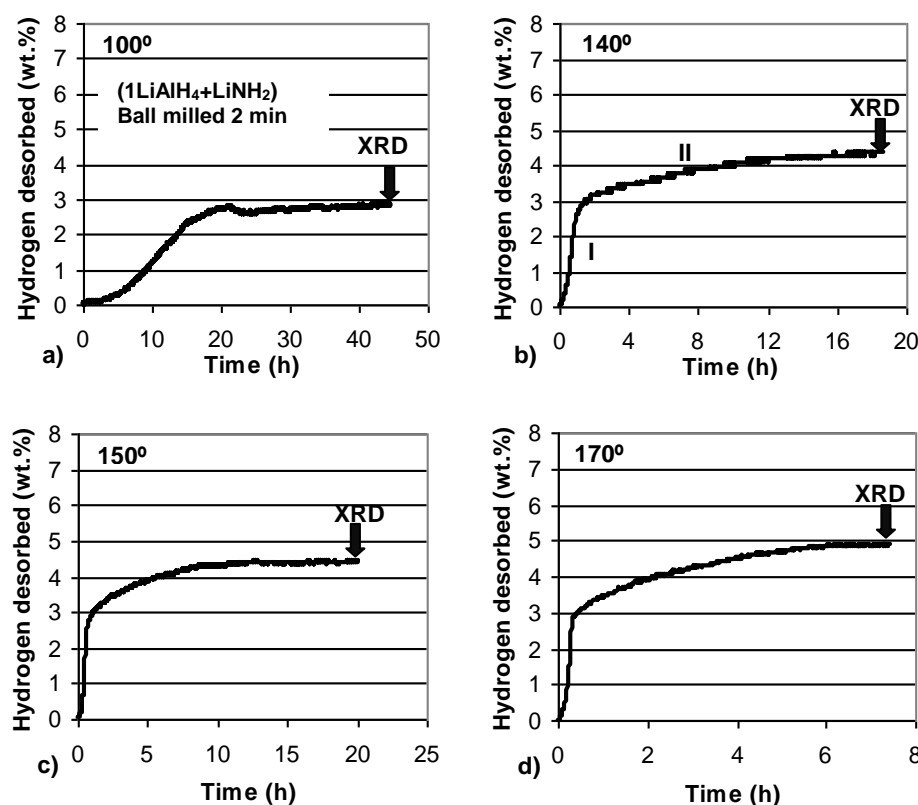
In order to investigate phase transformations occurring during isothermal dehydrogenation, the powder samples were extracted after completion of each desorption time as shown by the arrows in Figure 3 and were studied by XRD. Figure 4 shows the typical XRD patterns obtained after dehydrogenation at 100, 140 and 170 °C. As can be seen, the microstructure after dehydrogenation at 100 °C shows the presence of Li_3AlH_6, $LiNH_2$ and Al which indicate that reaction (1) is already completed since ~3 wt.% H_2 is desorbed (Figure 3a). After dehydrogenation at 140 °C, very weak principal diffraction peaks of Li_3AlH_6 are still visible together with strong Al peaks and basically unchanged $LiNH_2$ peaks. The quantity of ~4.4 wt.% H_2 desorbed (Figure 3b) indicates that reaction (2) is near completion. Finally, after completion of dehydrogenation at 170 °C no peaks of Li_3AlH_6 are visible while strong Al and $LiNH_2$ peaks are clearly seen. This microstructure corresponds to

desorption of 5 wt.% H_2 , as shown in Figure 3d, which means that both reactions (1) and (2) must have been completed. Since the total H_2 capacity of reactions (1) and (2) is about 5 wt.%, there is a perfect match between observed H_2 desorption capacities in Figure 3 and the microstructure in Figure 4 after dehydrogenation at 170 °C. Since there is no observed change in the intensities of the $LiNH_2$ peaks in Figure 4, which is a microstructural constituent during H_2 desorption, there is no reason to believe that any other reaction involving $LiNH_2$, other than reactions (1) and (2), occurred during dehydrogenation of the *n* = 1 composite up to 170 °C.

> **Figure 4.** XRD patterns for (1LiAlH$_4$ + LiNH$_2$) ball milled for 2 min and subsequently isothermally dehydrogenated at 100, 140 and 170 °C. The ICDD file numbers for phase identification are shown in the legend.
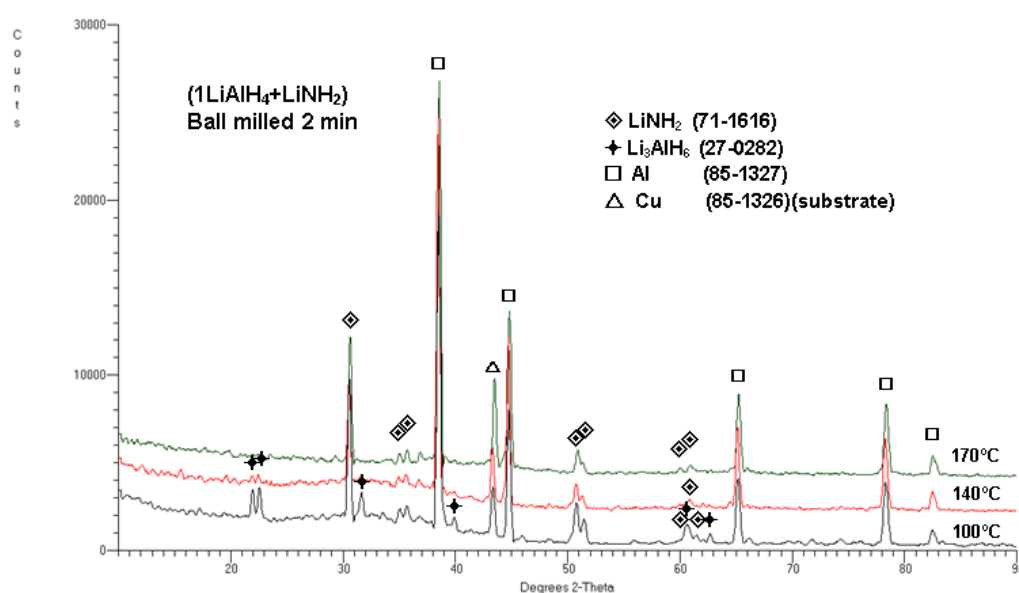
However, for the sake of clarity it must be pointed out that at high temperatures above 500 °C both Dolotko *et al.* [6] and Xiong *et al.* [7] reported that the reaction occurs between LiAlH$_4$ and LiNH$_2$ in a (0.5LiAlH$_4$ + LiNH$_2$) composite, as a result of which (Li$_3$AlN$_2$ + 4H$_2$) is formed, desorbing 9.5 wt.% H$_2$. As reported in [7] this reaction was reversible at about 350 °C under 80 bar H$_2$ pressure, providing about 5 wt.% H$_2$ according to the following reaction:

$$Li_3AlN_2 + 2H_2 \rightarrow LiNH_2 + 2LiH + AlN; \Delta H = -50.1 \text{ kJ mol}^{-1} H_2 \qquad (4)$$

On the other hand, Dolotko *et al.* [6] claimed that they rehydrogenated the fully decomposed (1LiAlH$_4$ + LiNH$_2$) mixture at 275 °C at 180 bar of H$_2$ pressure , supposedly according to reaction (4). The microstructure after rehydrogenation consisted of LiNH$_2$, metallic Al, LiH, amorphous Li$_3$AlN$_2$, amorphous AlN, and an unknown species "X". This microstructure does not exactly agree with reaction (4). Apparently, the establishing of dehydrogenation/rehydrogenation paths for the LiAlH$_4$-LiNH$_2$ composites at high temperatures and pressures still requires more research.

Figure 5 shows volumetric isothermal dehydrogenation curves at four temperatures for (11.5LiAlH$_4$ + LiNH$_2$) (a molar ratio corresponding to 5 wt.% LiNH$_2$) ball milled for 15 min. No desorption of H$_2$ during the 15 min milling is observed (Figure 1a) for this molar ratio. For the molar

ratio $n = 11.5$ (95 wt.% LiAlH$_4$), the purity-corrected H$_2$ capacity of reactions (1) and (2) is ~4.88 and 2.39 wt.%, respectively. The dehydrogenation curves exhibit the same two stages of desorption I and II as those in Figure 3 for the $n = 1$ composite. It is also clearly seen that at each temperature, the rate of H$_2$ desorption is much more rapid than that for the $n = 1$ composite in Figure 3. At 100 °C after a comparable time of 40 h the $n = 11.5$ composite desorbs nearly 6 wt.% H$_2$ (Figure 5a) as compared to barely ~3 wt.% H$_2$ for the $n = 1$ composite (Figure 3a). At 140, 150 and 170 °C the $n = 11.5$ composite desorbs ~7 wt.% H$_2$ which is nearly equal to the purity corrected total capacity of reactions (1) and (2) for 95 wt.% LiAlH$_4$ in the composite (~7.3 wt.% H$_2$).

Figure 5. Volumetric dehydrogenation curves at (**a**) 100 °C, (**b**) 140 °C, (**c**)150 °C and (**d**) 170 °C (at 1 bar H$_2$) for (11.5LiAlH$_4$ + LiNH$_2$) ball milled for 15 min. The arrows indicate the dehydrogenation time after which samples were taken for XRD tests.
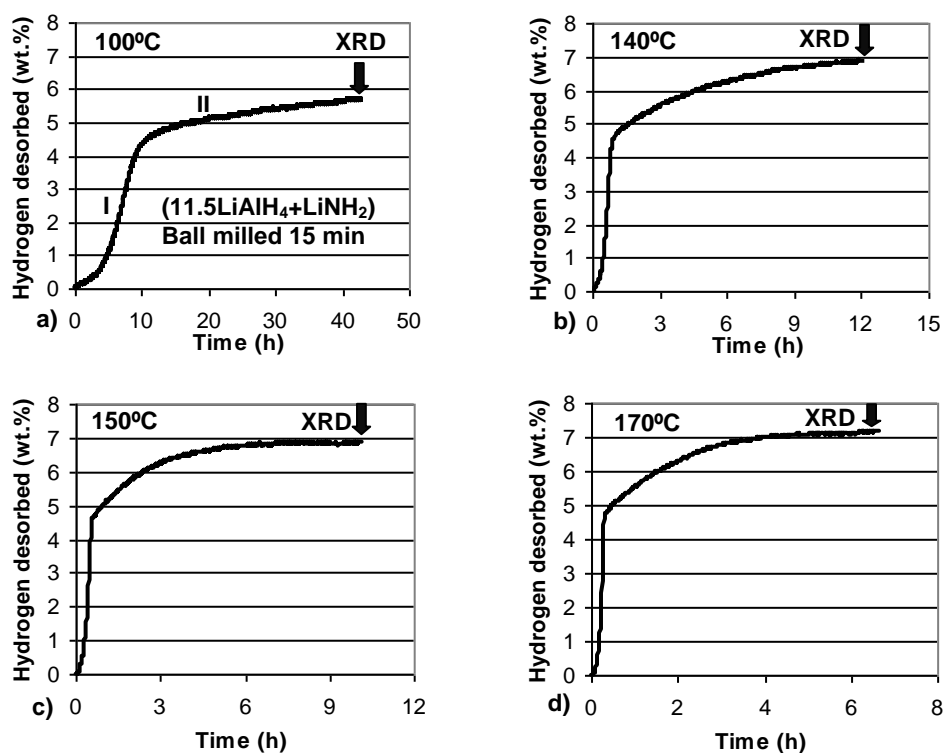
After completion of each desorption, the powder samples were extracted for XRD studies as indicated by the arrows in Figure 5. The XRD patterns in Figure 6 clearly confirm that the phase transformations occurred in accordance with reactions (1) and (2). After dehydrogenation at 100 °C there are clear peaks of Li$_3$AlH$_6$, and no peaks of LiAlH$_4$, confirming that reaction (1) is completed. However, the quantity of H$_2$ desorbed at this temperature is nearly 6 wt.% (Figure 5a) which also indicates that reaction (2) must have partially occurred. After dehydrogenation at 140 °C, weak peaks of Li$_3$AlH$_6$ are visible (Figure 6), which show that reaction (2) is near completion. At 170 °C, no peaks of Li$_3$AlH$_6$ are discernible, indicating the completion of reaction (2). For the sake of explanation, it must be pointed out that the occurrence of reaction (2) requires the presence of LiH in the microstructure. However, we were unable to identify the LiH peaks in the XRD patterns in Figure 4 and 6 after dehydrogenation at 140 and 170 °C. There is a common problem with finding LiH peaks in

the multiphase hydride/Al metal microstructures by XRD. First, the LiH Bragg peaks superimpose nearly completely with the Al peaks, because both have an FCC crystallographic structure and a very similar lattice parameter (one can compare ICDD 85-1327 for Al and 09-0340 for LiH). Second, as a very light hydride, LiH does not effectively diffract X-rays, particularly when metallic Al is present together with LiH and the low intensity LiH diffraction peaks are strongly suppressed by the high intensity Al peaks. Third, it may be at least partially amorphous after ball milling.

Figure 6. XRD patterns for $(11.5LiAlH_4 + LiNH_2)$ ball milled for 15 min and subsequently isothermally dehydrogenated at 100, 140 and 170 °C. The ICDD file numbers for phase identification are shown in the legend.
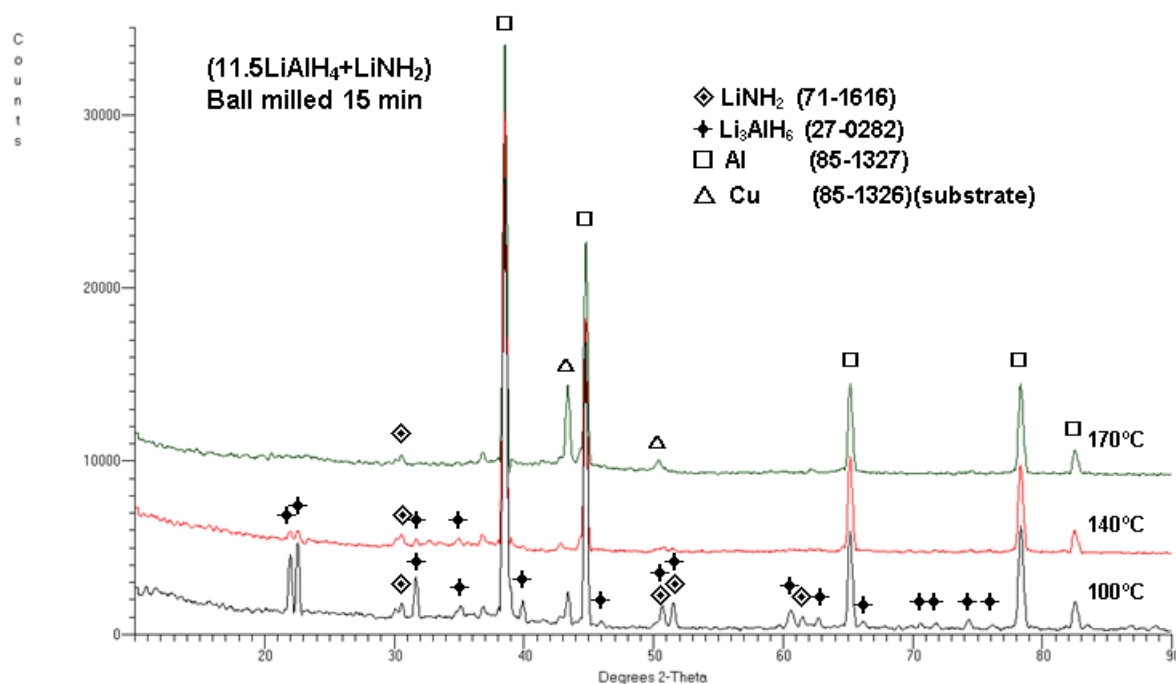
As shown earlier, $LiNH_2$ strongly enhances destabilization of $LiAlH_4$ in the $(1LiAlH_4 + LiNH_2)$ composite during ball milling (Figure 1b). One would expect that at the molar ratio $n = 1$, a similar destabilization effect might be observed during isothermal dehydrogenation. However, Figure 3 shows that this is not the case. Therefore, the question arises: why did $LiNH_2$ not enhance the dehydrogenation rate during isothermal dehydrogenation as observed in Figure 3? This is most likely related to a very short milling time of 2 min for the $(1LiAlH_4 + LiNH_2)$ composite which we used for processing. On one hand, such a short milling time prevents H_2 release during milling (Figure 1b) allowing subsequent dehydrogenation of the full H_2 capacity of the $n = 1$ composite (Figure 3). On the other hand, the milling time of 2 min is most likely too short to allow for an intimate hydride phase alloying and substantial nanostructuring of the composite such as reduction of particle and crystallite (grain) size within the particles. It is well known that nanostructuring, and especially the reduction of powder particle size, is one of the critical factors enhancing dehydrogenation/rehydrogenation properties of hydrides and their composites [2]. We observe that both $LiAlH_4$ and $LiNH_2$ are not particularly prone to nanostructuring. We reported for $LiAlH_4$ that a high energy milling duration for 20 h reduced its initial particle size from 9.9 ± 5.2 μm to 2.8 ± 2.3 μm [11], still far away from a

nanometric range. The crystallite (grain) size of $LiAlH_4$ actually slightly increased from ~30 nm to ~80 nm range after 15 min of high energy ball milling [11]. We also reported that high energy ball milling of $LiNH_2$ for 1 h changed its Specific Surface Area (SSA) only slightly for particle sizes from 16.5 to 26.4 m^2/g with an associated crystallite (grain) size still at ~65 nm [16]. Therefore, it is quite clear that a short milling time for just 2 min might have been insufficient for any substantial refinement of microstructure that, in turn, would lead to improvement of thermal dehydrogenation for the $n = 1$ composite.

In contrast, a continuous high energy ball milling for a few hours was, most likely, sufficient to refine microstructure and allow dehydrogenation of full H_2 capacity from the $n = 1$ composite (Figure 1b) after 100–150 min in the presence of $LiNH_2$, destabilizing $LiAlH_4$. Apparently, the $(1LiAlH_4 + LiNH_2)$ composite creates a serious dilemma for the enhancement of its dehydrogenation properties at elevated temperatures because it definitely needs a longer milling time than just 2 min to bring about more structural refinement. In turn, a longer milling time leads to a loss of H_2 during milling (Figure 1b). One possible avenue to overcome this problem could be ball milling of both constituents $LiAlH_4$ and $LiNH_2$ separately for sufficient time to achieve their microstructural refinement and then composite them together by relatively short ball milling.

As can be seen in Figure 5, for the $n = 11.5$ composite, its thermal dehydrogenation rate increases as compared to the $n = 1$ composite (Figure 3), most likely due to an enhanced microstructural refinement resulting from a longer high energy milling time which does not lead to H_2 desorption during milling at molar ratios >3. The dehydrogenation behavior at 100 ℃ of a composite with $n = 11.5$, which corresponds to 5 wt.% content of $LiNH_2$, is compared in Figure 7 to the dehydrogenation behavior of single phase $LiAlH_4$ and to the dehydrogenation behavior of the composite of $LiAlH_4$, containing 5 wt.% of a nanometric Ni catalyst whose hydrogen storage properties were reported in [12]. All composites were ball milled for 15 min under the same milling conditions. Apparently, the ball milled $(11.5LiAlH_4 + LiNH_2)$ composite exhibits a more rapid dehydrogenation rate in stage I (reaction (1)) than a simple ball milled single phase $LiAlH_4$. However, in stage II (reaction (2)) both have nearly identical dehydrogenation rates, although the rates for both are much inferior to the dehydrogenation rate of ball milled $LiAlH_4$ catalyzed with 5 wt.% n-Ni (curve c): the latter being the same weight content as that for $LiNH_2$ in the $n = 11.5$ composite. This comparison shows that a small content of $LiNH_2$ composited with $LiAlH_4$ enhances rather modestly the thermal dehydrogenation rate of the $LiAlH_4$ constituent in the composite.

Figure 7. A comparison of dehydrogenation curves at 100 ℃ (at 1 bar H_2) for the following composites ball milled under the same conditions: a- $LiAlH_4$, b- ($11.5LiAlH_4$ + $LiNH_2$) (5 wt.% $LiNH_2$) composite and c- ($LiAlH_4$ + 5 wt.% n-Ni) (n-Ni-nanometric size Ni catalyst). Curve c is re-plotted from [12].
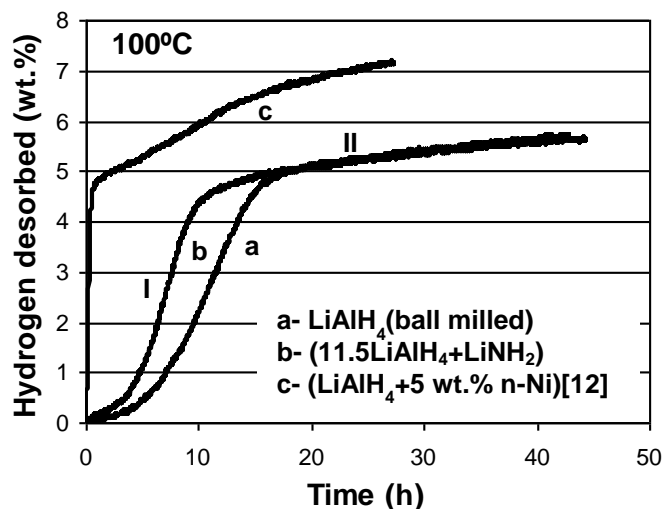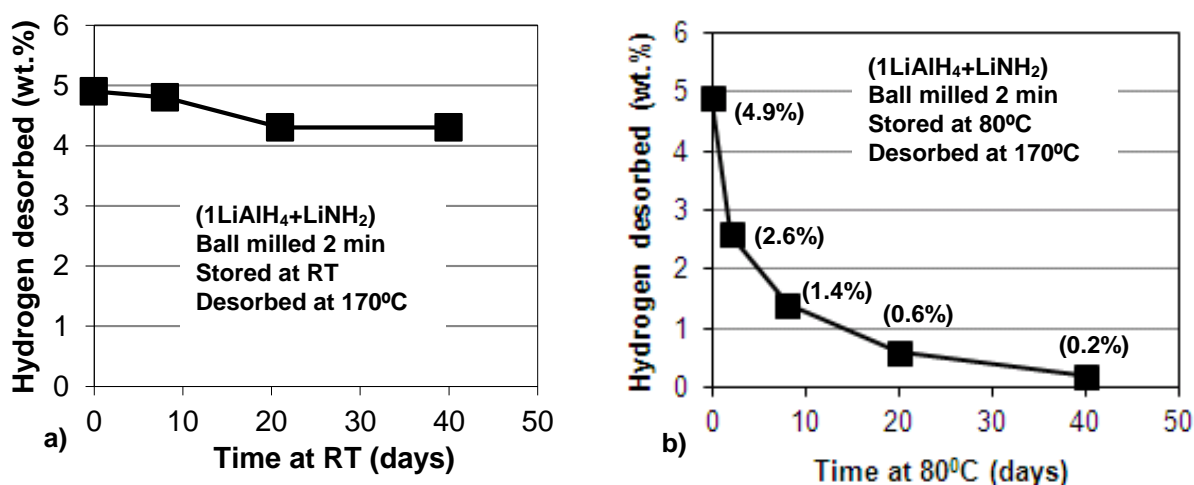

Figure 8. Plot of hydrogen desorbed at 170 ℃ vs. storage time at (**a**) room temperature (RT) and (**b**) 80 ℃, in days (1 day = 24 h) for the ($1LiAlH_4$ + $LiNH_2$) composite ball milled for 2 min. Stored under Ar; subsequently, fully dehydrogenated at 170 ℃ at 1 bar H_2 pressure. The numbers in parentheses show the quantity of H_2 desorbed isothermally at 170 ℃.


Recently, we reported that ball milled $LiAlH_4$ catalyzed with nanometric Ni (n-Ni), slowly discharged during storage at room temperature, 40 and 80 ℃, gradually releasing quite substantial quantities of H_2 [12]. In the present work, we also investigated long term dehydrogenation of the ($1LiAlH_4$ + $LiNH_2$) composite, ball milled for only 2 min (no H_2 release during milling). The composite was stored after ball milling in a sealed glass vial containing high purity Ar under slight overpressure temperature in a glove box and in an oven at 80 ℃. After a pre-determined length of time small samples of stored composite were extracted from the vial and fully dehydrogenated isothermally at 170 ℃ in a Sieverts-type apparatus at 1 bar H_2 pressure, registering the quantity of H_2 desorbed. At room temperature, the composite discharged about 0.6 wt.% H_2 after 40 days of storage (Figure 8a).

However, at 80 °C the dehydrogenation rate dramatically accelerated, as shown in Figure 8b. It is observed that after 40 days of storage the H_2 discharge during storage amounts to ~4.7 wt.% H_2 which, practically, is the total capacity of reactions (1) and (2) for the molar ratio *n* = 1 (3.2 and 1.6 wt.% H_2, respectively).

In order to understand the microstructural evolution which occurs during slow desorption at 80 °C, small samples for XRD were extracted after 8, 20 and 40 days. The corresponding XRD patterns obtained from the extracted samples are shown in Figure 9. After 8 days of storage, the weak peaks of Li_3AlH_6 and strong principal peaks of phases such as Al and $LiNH_2$ are observed. After 20 and 40 days, the Li_3AlH_6 peaks are barely visible and very strong peaks of Al and $LiNH_2$ are clearly observed. Figure 8b shows that during the first 8 days of storage, the sample discharged ~3.5 wt.% H_2, and during the next 32 days, the sample discharged an additional 1.2 wt.% H_2 to the total of 4.7 wt.% H_2. Apparently, the highest rate of dehydrogenation is observed for the first few days of storage. It is perfectly clear that the slow dehydrogenation during long term storage occurs up to 8 days mostly by reaction (1), and possibly the early stage of reaction (2), and then it proceeds by reaction (2). The persistent presence of the $LiNH_2$ peaks indicates that this hydride is not involved in any other auxiliary reactions at room temperature.

Figure 9. XRD patterns obtained for the ball milled (1$LiAlH_4$ + $LiNH_2$) composite, stored at 80 °C under Ar for 8, 20 and 40 days (1 day = 24 h). The ICDD file numbers for phase identification are shown in the legend.
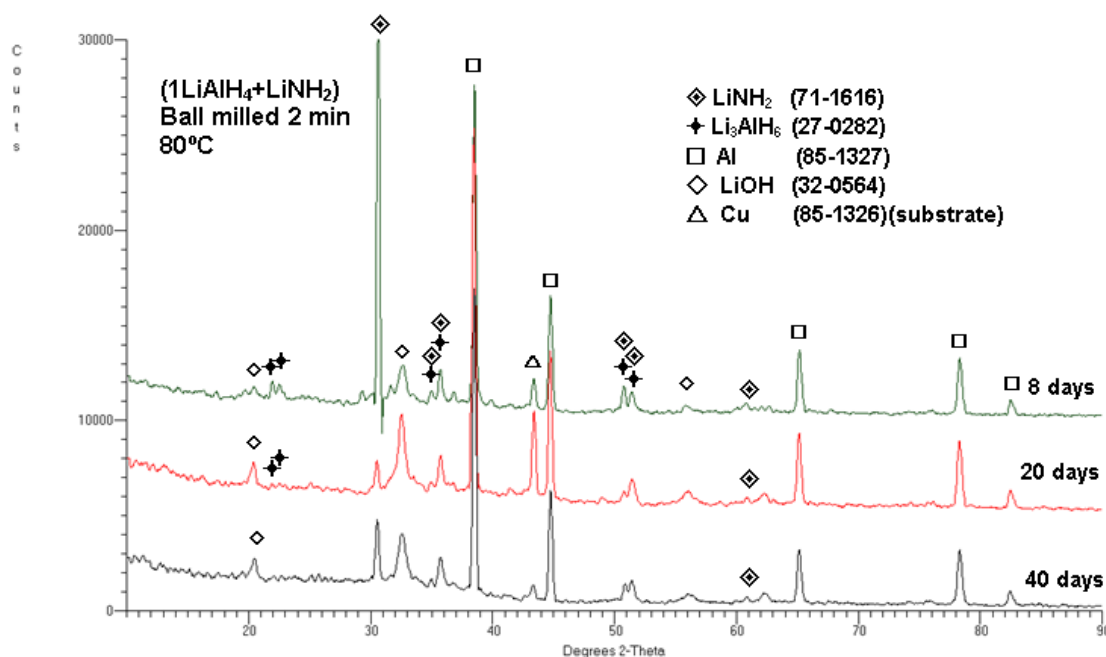
Finally, it must be pointed out that the diffraction peaks of LiOH are also observed in the XRD patterns in Figure 9. LiOH is an impurity, frequently found in $LiNH_2$ [16]. Alternatively, a part of LiOH might have been formed by oxidation of LiH from reaction (2) in an XRD holder.

4. Conclusions

Hydrogen storage properties of the (nLiAlH$_4$ + LiNH$_2$; n = 1, 3, 11.5 and 30) composites synthesized by high energy ball milling have been investigated. The major conclusions are as follows:

(1) The composite with the molar ratio n = 1 releases nearly 4 wt.% H$_2$ after the first 30 min of ball milling and up to nearly 5 wt.% H$_2$ after 180 min.

(2) For the n = 3 composite, the quantity of H$_2$ released is only ~0.6 wt.% for the first 30 min of milling. The composites with the molar ratio n = 11.5 and 30 do not release H$_2$ during ball milling.

(3) The XRD studies of microstructural changes occurring during ball milling convincingly indicate that the H$_2$ release is simply provided by a solid state decomposition of LiAlH$_4$ into (1/3)Li$_3$AlH$_6$ + (2/3)Al + H$_2$ (reaction (1) and subsequently (1/3)Li$_3$AlH$_6$ into LiH + Al + 0.5H$_2$ (reaction (2)).

(4) Most interestingly, in a thermal DSC test, reaction (1) is exothermic and reaction (2) is endothermic, but both are induced by ball milling at close to room temperature.

(5) No convincing evidence of any reaction involving LiNH$_2$ has been found. Both reactions of LiAlH$_4$ decomposition during ball milling are enhanced by the presence of a large amount of LiNH$_2$ (37.7 wt.%) in the n = 1 composite which strongly destabilizes LiAlH$_4$. It does not seem that LiNH$_2$ acts as a typical catalytic additive. However, the exact mechanism is unclear at the moment.

(6) Reducing the content of LiNH$_2$ in the composite by increasing the molar ratio of LiAlH$_4$ to 3, 11.5 and 30, substantially weakens the destabilizing effect of LiNH$_2$ on the decomposition of LiAlH$_4$ during ball milling.

(7) The n = 1 composite, ball milled for only 2 min to avoid loss of H$_2$ during milling, exhibits sluggish dehydrogenation rates at the temperature range 100–170 °C. This behavior is most likely due to insufficient microstructural refinement (particle and grain size) induced by too short a milling time.

(8) The n = 11.5 (5 wt.% LiNH$_2$) composite, ball milled for 15 min, which provides enhanced microstructural refinement, is able to desorb 6–7 wt.% H$_2$ in the temperature range 100–170 °C. However, its rate of dehydrogenation is still lower than that for the composite of LiAlH$_4$ catalyzed with 5 wt.% n-Ni, ball milled under the same conditions and investigated in [12].

(9) XRD studies indicate that isothermal dehydrogenation (nLiAlH$_4$ + LiNH$_2$) occurs by the same decomposition reactions of LiAlH$_4$ as those during ball milling.

(10) The n = 1 composite, ball milled for 2 min and subsequently stored for longer time under Ar at 80 °C, slowly discharges large quantities of H$_2$ approaching 3.5 wt.% after 8 days of storage.

References

1. Dillich, S. *D.O.E. Hydrogen Program 2009 Annual Progress Report*; Technical Report for IV.0 Hydrogen Storage Sub-Program Overview: U.S. Department of Energy, Washington, DC, USA, May 2009.

2. Varin, R.A.; Czujko T.; Wronski, Z.S. *Nanomaterials for Solid State Hydrogen Storage*, Springer Science & Business Media: New York, NY, USA, 2009.

3. Lu, J.; Fang, Z.Z. Dehydrogenation of a combined $LiAlH_4/LiNH_2$ system. *J. Phys. Chem.* **2005**, *109*, 20830–20834.

4. Chen, R.; Wang, X.H.; Chen, L.X.; Li, S.Q.; Ge, H.W.; Lei, Y.Q.; Chen, X.P. An investigation on the reaction pathway between $LiAlH_4$ and $LiNH_2$ via gaseous ammonia. *J. Alloys Compd.* **2010**, *495*, 17–22.

5. Naik, M.; Rather, S.; So, C.S.; Hwang, S.W.; Kim, A.R.; Nahm, K.S. Thermal decomposition of $LiAlH_4$ chemically mixed with lithium amide and transition metal chlorides. *Int. J. Hydrogen Energy* **2009**, *34*, 8937–8943.

6. Dolotko, A.; Kobayashi, T.; Wiench, J.W.; Pruski, M.; Pecharsky, V. Investigation of the thermochemical transformations in the $LiAlH_4$-$LiNH_2$ system. *Int. J. Hydrogen Energy* **2011**, *36*, 10626–10634.

7. Xiong, Z.T.; Wu, G.T.; Hu, J.J.; Chen, P. Investigation on chemical reaction between $LiAlH_4$ and $LiNH_2$. *J. Power Sources* **2006**, *159*, 167–170.

8. Xiong, Z.T.; Wu, G.T.; Hu, J.J.; Liu, Y.F.; Chen, P.; Luo, W.F.; Wang, J. Reversible hydrogen storage by a Li-Al-N-H complex. *Adv. Funct. Mater.* **2007**, *17*, 1137–1142.

9. Nakamori, Y.; Ninomiya, A.; Kitahara, G.; Aoki, M.; Noritake, T.; Miwa, K.; Kojima, Y.; Orimo, S. Dehydriding reactions of mixed complex hydrides. *J. Power Sources* **2006**, *155*, 447–455.

10. Dolotko, O.; Zhang, H.Q.; Ugurlu, O.; Wiench, J.W.; Pruski, M.; Chumbley, L.S.; Pecharsky, V. Mechanochemical transformations in Li(Na)AlH_4-Li(Na)NH_2 systems. *Acta Mater.* **2007**, *55*, 3121–3130.

11. Varin, R.A.; Zbroniec, L. Decomposition behavior of unmilled and ball milled lithium alanate ($LiAlH_4$) including long-term storage and moisture effects. *J. Alloys Compd.* **2010**, *504*, 89–101.

12. Varin, R.A.; Zbroniec, L. The effects of nanometric nickel (Ni) catalyst on the dehydrogenation and rehydrogenation behavior of ball milled lithium alanate ($LiAlH_4$). *J. Alloys Compd.* **2010**, *506*, 928–939.

13. Varin, R.A.; Zbroniec, L.; Czujko, T.; Wronski, Z.S. The effects of nanonickel additive on the decomposition of complex metal hydride $LiAlH_4$ (lithium alanate). *Int. J. Hydrogen Energy* **2011**, *36*, 1167–1176.

14. Varin, R.A.; Zbroniec, L. The effects of ball milling and nanometric nickel additive on the hydrogen desorption from lithium borohydride and manganese chloride ($3LiBH_4+MnCl_2$). *Int. J. Hydrogen Energy* **2010**, *35*, 3588–3597.

15. Varin, R.A.; Czujko, T.; Wronski, Z.S. Thermal stability of Vale Inco nanometric nickel as a catalytic additive for magnesium hydride (MgH_2). *Int. J. Hydrogen Energy* **2009**, *34*, 8603–8610.

16. Varin, R.A.; Jang, M.; Polanski, M. The effects of ball milling and molar ratio of LiH on the hydrogen storage properties of nanocrystalline lithium amide and lithium hydride (LiNH$_2$+LiH) system. *J. Alloys Compd*. **2010**, *491*, 658–667.